

A Cap–Axis Integral Diagnostic of Factor Models

Useong Shin*

July 3, 2026

JEL: G12; G11; C52; C58

Keywords: factor models; asset pricing tests; stochastic discount factor; market capitalization; pricing errors; model evaluation

Abstract

I propose a *cap-axis integral diagnostic* for factor-model evaluation. Low-dimensional factor models can improve the maximum-Sharpe frontier while leaving zero-alpha violations on economically fixed subspaces. The diagnostic studies one such subspace by lifting pricing errors into a bridge-alpha curve along the market-capitalization rank axis. Under an aggregate-market gate, a zero curve is equivalent to pricing the market's internal cap-rank subspace. In 1967–2024 CRSP data, q5's daily negative bridge attenuates under lead–lag correction, while Fama–French and Carhart bridges are more visible monthly. Across 154 factors, the cap-axis norm is distinct from Sharpe gain and size exposure.

*Sogang Business School, Sogang University (Seoul, Korea).
ORCID: [0009-0003-0197-9003](https://orcid.org/0009-0003-0197-9003)
Email: useong@sogang.ac.kr

1 Introduction

In the ideal SDF problem, zero-alpha pricing and mean–variance efficiency are two views of the same object. A correctly specified SDF prices every payoff, and the associated tangency portfolio attains the relevant maximum Sharpe ratio. Empirical factor models are low-dimensional approximations. For them, the two criteria can separate: a factor span can improve the maximum–Sharpe frontier while leaving systematic pricing errors on an economically meaningful subspace.

This separation is not a new theoretical impossibility result; it is already implicit in standard alpha–spanning logic. The contribution of this paper is to make the separation measurable on a fixed economic coordinate. I propose a *cap-axis integral diagnostic* that lifts factor-model pricing errors into a curve along the market-capitalization rank axis inside the market portfolio. Standard tests usually compress misspecification into a verdict: a model prices a chosen test-asset set, spans another model, or improves a scalar loss. These tests are useful, but they do not show where pricing errors live.

The construction is simple. Sort investable stocks by descending market capitalization. For each cumulative-cap share p , form a zero-investment bridge by going long the top- p prefix and shorting an equal market-value exposure of the aggregate market. Regressing this bridge return on a factor model gives an alpha, $\alpha_m(p)$. Varying p produces a *bridge-alpha curve*, closed at $p = 0$ and $p = 1$ by construction.

The curve has a direct pricing interpretation. Under an aggregate-market consistency gate—the model prices the aggregate market—a zero bridge-alpha curve is necessary and sufficient for the model to price the closed linear subspace generated by the market and all cap-axis bridges ([Proposition 1](#)). This subspace contains every cap-rank prefix, tail, interval, and step-function portfolio generated by the axis. Passing the diagnostic is therefore stronger than pricing any fixed finite set of size portfolios on this coordinate: it means pricing the market’s internal cap-rank subspace.

The diagnostic is intentionally restricted. It does not test all anomaly, industry, momentum, value, profitability, investment, or idiosyncratic long–short directions. Its value is that it fixes one market-internal coordinate with little test-asset discretion and measures the pricing-error shape along it. I summarize the curve by a signed area \widehat{SA} and three functional norms, \widehat{IAE} , \widehat{ISE} , and \widehat{SUP} , which separate direction, total magnitude, and local distortion. The signed area also equals the alpha of a single rank-area portfolio in the continuous population and is nearly identical on the finite grid ([Section 4.4.1](#)).

I apply the diagnostic to the CRSP investable market from 1967 to 2024. All models first pass the aggregate-market gate. The cap-axis diagnostic then reveals frequency-localized

pricing errors that the aggregate check cannot show. At the daily frequency, q5 displays a one-sided negative bridge-alpha curve that attenuates under lead-lag correction. At the monthly frequency, q5’s large daily bridge is nearly absent, while the Fama–French and Carhart models display positive cap-axis bridges. The result is not a model ranking. It shows that approximate SDFs can place their cap-rank pricing errors at different horizons.

I use ordering placebos as matched benchmarks for cap-rank specificity. They hold dates, returns, market weights, split shares, and estimation design fixed while removing only the capitalization-rank ordering. I also scan 154 monthly factors, formed from the [Jensen et al. \(2023\)](#) anomaly library and the Fama–French and q -factor series, by adding each factor to the market and measuring its cap-axis footprint ([Section 6](#)). The footprint is distinct from both maximum-Sharpe gain and size exposure: rank correlations with Sharpe improvement are low, and size-loading R^2 is close to zero.

The paper therefore adds a restricted zero-alpha complement to joint alpha tests, spanning tests, and maximum-Sharpe-ratio comparisons. A model can pass the aggregate market, expand the mean–variance frontier, and still leave a nonzero bridge-alpha curve on the cap-rank subspace. Conversely, a model can have a small curve on this axis while leaving errors elsewhere. The diagnostic recovers the direction, magnitude, location, and frequency of pricing errors along a fixed market-internal coordinate.

The remainder of the paper proceeds as follows. [Section 2](#) reviews related work. [Section 3](#) defines the cap-axis bridge and pricing proposition. [Section 4](#) describes the data and implementation. [Section 5](#) reports the daily and monthly results. [Section 6](#) maps factors onto the cap-axis coordinate. [Section 7](#) presents robustness checks. [Section 8](#) contrasts the diagnostic with size-decile tests. [Section 9](#) discusses interpretation and limitations, and [Section 10](#) concludes.

2 Theoretical Background and Related Literature

Model comparison criteria. The expansion of multifactor models has made model comparison a central issue in empirical asset pricing. Standard candidates include the Fama–French models ([Fama and French, 1992, 1993, 2015](#)), momentum ([Jegadeesh and Titman, 1993; Carhart, 1997](#)), and the investment-and-profitability q -factor family and its anomaly-replication applications ([Hou et al., 2015, 2019, 2020, 2021, 2024](#)). A leading comparison criterion is factor spanning and the associated maximum-Sharpe-ratio frontier ([Barillas and Shanken, 2017, 2018; Fama and French, 2018](#)): a model is evaluated by whether its factor span improves the attainable mean–variance opportunity set.

This paper does not replace that criterion. It studies a complementary object. A factor

span can expand the mean–variance frontier while leaving pricing errors on a fixed economic subspace. The cap-axis diagnostic measures such errors on one subspace: the market portfolio’s internal capitalization–rank axis.

Test-asset dependence. Joint alpha tests and distance measures depend on the chosen test assets (Gibbons et al., 1989; Hansen and Jagannathan, 1997; Cochrane, 2005). Test-portfolio construction can therefore affect inference and rankings (Lewellen et al., 2010), especially with weak factors, redundant factors, or repeated model search (Giglio et al., 2025; Kozak et al., 2018; Lo and MacKinlay, 1990). Maximum–Sharpe comparisons reduce this dependence by focusing on the factor span. The cap-axis diagnostic takes the opposite route: it keeps the zero-alpha question but fixes the test-asset coordinate. The test assets are zero-investment bridges comparing each cumulative capitalization–rank prefix with an equal-exposure aggregate market. The coordinate is therefore generated by the market portfolio’s own capitalization weights, not by an anomaly sort chosen ex post.

Characteristic-sorted portfolios as functions. The diagnostic is closest in spirit to work that treats characteristic-sorted portfolio returns as functions over a characteristic domain. Cattaneo et al. (2020) develop estimation and inference for characteristic-sorted portfolios. I apply this functional view to market-capitalization rank and to a specific object, the bridge-alpha curve. Instead of testing only a finite set of pointwise alphas, I summarize the curve by a signed area and by *IAE*, *ISE*, and *SUP* norms, which separate direction, total magnitude, and local extremity of pricing errors along the cap–rank coordinate.

Factor coordinates. The factor-coordinate exercise uses the replicated anomaly factors of Jensen et al. (2023), distributed through Global Factor Data (Global Factor Data, 2026), augmented with the Fama–French/Carhart and q -factor series used elsewhere in the paper. This broad factor set allows the cap-axis footprint to be compared with familiar coordinates such as maximum–Sharpe gain and size exposure. The exercise is descriptive: it asks whether the cap-axis norm is a restatement of existing factor coordinates or a distinct feature of factor behavior.

Frequency and non-synchronous trading. Daily factor regressions can be affected by non-synchronous trading. If small or illiquid stocks react to market-wide information with a lag, daily beta estimates can be attenuated and intercepts distorted. The lead–lag corrections of Scholes and Williams (1977) and Dimson (1979) address this issue by aggregating lagged and leading factor loadings. I apply the same logic to the cap-axis bridge. Varying the

lead-lag window produces a horizon profile of the signed-area alpha and helps distinguish short-horizon attenuation from lower-frequency pricing-error structure.

Relation to closely related work. The paper extends two closely related designs. [Shin \(2026a\)](#) uses random portfolios as matched benchmarks for factor-model pricing tests. Here, ordering placebos apply the same principle to capitalization rank: dates, returns, market weights, and split shares are held fixed while only the stock order is randomized. [Shin \(2026b\)](#) studies selected body-tail splits of the market. This paper replaces those scalar splits with a bridge-alpha function over the entire cumulative-cap axis. A body-tail split is one point on the curve; the cap-axis diagnostic estimates the whole path and summarizes it by functional statistics.

3 Cap-Axis Integral Diagnostic

This section defines the cap-axis integral diagnostic. The object is a pricing-error path generated by traversing the market portfolio in capitalization-rank order. It is restricted by design: it does not test full SDF validity, but pricing consistency on the subspace generated by the aggregate market and cap-axis bridge portfolios.

3.1 A pricing-error bridge along the market-value axis

Fix a date t and sort assets by descending market capitalization at the previous formation date. Let $u \in [0, 1]$ denote cumulative market-value rank, normalized so that du represents market-value share. Let $r_t(u)$ be the simple return of the infinitesimal portfolio at rank u . The aggregate market return is

$$R_t^M = \int_0^1 r_t(u) du. \tag{1}$$

For cutoff $p \in [0, 1]$, define the top- p market-value contribution as

$$C_t(p) = \int_0^p r_t(u) du. \tag{2}$$

The cap-axis bridge longs this prefix and shorts an equal market-value exposure of the aggregate market:

$$D_t(p) = C_t(p) - pR_t^M. \tag{3}$$

The bridge is zero at both endpoints,

$$D_t(0) = D_t(1) = 0, \quad (4)$$

and the corresponding tail bridge satisfies

$$D_t^T(p) = \int_p^1 r_t(u) du - (1-p)R_t^M = -D_t(p). \quad (5)$$

Thus a single prefix bridge captures the body–tail offset at every cutoff.

For model m with factor vector $f_{m,t}$, estimate

$$D_t(p) = \alpha_m(p) + \beta_m(p)' f_{m,t} + \varepsilon_{m,t}(p). \quad (6)$$

The function $p \mapsto \alpha_m(p)$ is the *bridge-alpha curve*. The cap-axis null is

$$\alpha_m(p) = 0, \quad p \in [0, 1]. \quad (7)$$

I summarize the curve by four functionals:

$$SA_m = \int_0^1 \alpha_m(p) dp, \quad IAE_m = \int_0^1 |\alpha_m(p)| dp, \quad (8)$$

$$ISE_m = \int_0^1 \alpha_m(p)^2 dp, \quad SUP_m = \sup_{p \in [0,1]} |\alpha_m(p)|. \quad (9)$$

SA_m measures directional tilt. IAE_m and ISE_m measure total distortion without sign cancellation. SUP_m records the largest local distortion. Sample counterparts are denoted \widehat{SA}_m , \widehat{IAE}_m , \widehat{ISE}_m , and \widehat{SUP}_m .

3.2 Restricted cap-axis pricing

The bridge-alpha curve has a restricted pricing interpretation. Let R_M^e be the market excess return. Since $D(p)$ is zero-investment, it is already an excess return. Define

$$\mathcal{V}_{cap} = \overline{\text{span}} \{R_M^e, D(p) : p \in [0, 1]\} \quad (10)$$

as the L^2 closed linear span generated by the market and the cap-axis bridges.

Assumption 1 (Regularity). *All test returns and factor returns have finite second moments, and $\text{Var}(f_m)$ is nonsingular.*

Proposition 1 (Restricted cap-axis pricing). *Under [Assumption 1](#), model m prices every return in \mathcal{V}_{cap} if and only if*

$$\alpha_m(R_M^e) = 0 \quad \text{and} \quad \alpha_m(D(p)) = 0 \quad \text{for all } p \in [0, 1]. \quad (11)$$

Proof. For any $R \in L^2$, the OLS alpha functional is

$$\alpha_m(R) = \mathbb{E}[R] - \mathbb{E}[f_m]' \text{Var}(f_m)^{-1} \text{Cov}(f_m, R). \quad (12)$$

Under [Assumption 1](#), this is a bounded linear functional on L^2 . Necessity is immediate. For sufficiency, the condition sets the functional to zero on the generators of \mathcal{V}_{cap} . Linearity gives zero alpha on all finite linear combinations, and continuity extends the result to the closed span. \square

The proposition is a bookkeeping result; the economic restriction is the choice of generators. Passing the diagnostic means that, conditional on pricing the aggregate market, the model also prices every cap-rank prefix, tail, interval, and step-function portfolio generated by this axis. It says nothing about directions outside this subspace.

3.3 The rank-area portfolio

The signed area can be implemented as one zero-investment return. Integrating the bridge over p gives

$$\int_0^1 D_t(p) dp = \int_0^1 \left\{ \int_0^p r_t(u) du - pR_t^M \right\} dp \quad (13)$$

$$= \int_0^1 \left(\frac{1}{2} - u \right) r_t(u) du. \quad (14)$$

Define the rank-area return

$$Y_t = \int_0^1 \left(\frac{1}{2} - u \right) r_t(u) du. \quad (15)$$

Then

$$Y_t = \int_0^1 D_t(p) dp. \quad (16)$$

Because the OLS intercept is linear in the dependent variable,

$$\alpha_m(Y) = \int_0^1 \alpha_m(p) dp = SA_m. \quad (17)$$

The signed area is therefore the alpha of a single rank-area portfolio. This portfolio is not a size factor at one cutoff; its weight $1/2 - u$ integrates the whole bridge path.

3.4 Finite-asset implementation

In the data the market-value axis is observed through finitely many stocks. On date t , sort the investable universe by descending market capitalization and index stocks by $i = 1, \dots, N_t$. Let $w_{i,t}$ be the implemented market-value weight and $R_{i,t}$ the stock return:

$$\sum_{i=1}^{N_t} w_{i,t} = 1, \quad R_t^M = \sum_{i=1}^{N_t} w_{i,t} R_{i,t}. \quad (18)$$

Define cumulative share and midpoint rank as

$$c_{i,t} = \sum_{j=1}^i w_{j,t}, \quad \mu_{i,t} = c_{i,t} - \frac{1}{2} w_{i,t}. \quad (19)$$

For cutoff p , let

$$k_t(p) = \begin{cases} 0, & p = 0, \\ \min\{i : c_{i,t} \geq p\}, & p \in (0, 1], \end{cases} \quad s_t(p) = \begin{cases} 0, & p = 0, \\ c_{k_t(p),t}, & p \in (0, 1]. \end{cases} \quad (20)$$

The discrete bridge is

$$D_t(p) = \sum_{i=1}^{k_t(p)} w_{i,t} R_{i,t} - s_t(p) R_t^M. \quad (21)$$

This implementable return longs the whole-stock prefix and shorts the aggregate market at the same realized exposure $s_t(p)$. Endpoint closure remains exact, while p and $s_t(p)$ need not coincide because boundary stocks are not split.

At each cutoff, estimate

$$D_t(p) = \alpha_m(p) + \beta_m(p)' f_{m,t} + \varepsilon_{m,t}(p). \quad (22)$$

On a finite grid $\mathcal{P} = \{p_1, \dots, p_L\}$, the four curve statistics are computed by numerical integration and a grid maximum.

The discrete rank-area return is

$$Y_t = \sum_{i=1}^{N_t} w_{i,t} R_{i,t} \left(\frac{1}{2} - \mu_{i,t} \right). \quad (23)$$

It is the midpoint approximation to [Equation \(15\)](#). In the finite-stock implementation, its equality with the integrated bridge is approximate because bridge returns use whole-stock prefixes. I measure this boundary-quantization error directly in the empirical implementation.

Proposition 2 (Discrete restricted cap-axis pricing). *In a finite-asset market, if the aggregate-market alpha is zero and $\alpha_m(D(p)) = 0$ for every implemented bridge $p \in \mathcal{P}$, then model m prices the finite-dimensional span generated by the aggregate market and the implemented bridge returns.*

Proof. The result follows immediately from the linearity of the OLS alpha functional in [Equation \(12\)](#). □

4 Data and Methodology

This section describes the empirical implementation. I construct the CRSP investable market, verify the aggregate-market consistency gate, and specify the formation, frequency, inference, and placebo choices used to estimate the cap-axis bridge-alpha curve.

4.1 Constructing the CRSP investable universe

I use CRSP individual-stock data ([CRSP, 2026](#)), the Fama–French Data Library ([French, 2026](#)), and the q-factor provider data ([Global-q.org, 2026](#)). The stock-level sample runs from January 3, 1967 to December 31, 2024. The base universe consists of NYSE, AMEX, and NASDAQ common stocks. The filter removes the extreme microcap and illiquidity tail while preserving almost all of the market’s economic weight.

Investability is updated at each month-end using market capitalization and liquidity. The month-end market capitalization of stock i is

$$ME_{i,t} = |PRC_{i,t}| \times SHROUT_{i,t} \times 1,000. \tag{24}$$

After sorting stocks in descending ME , the cumulative market-cap share of stock i is

$$CumME_{i,t} = \frac{\sum_{j:ME_{j,t} \geq ME_{i,t}} ME_{j,t}}{\sum_j ME_{j,t}}. \tag{25}$$

Liquidity is measured by average dollar volume over the most recent 63 trading days:

$$DVOL_{i,d} = |PRC_{i,d}| VOL_{i,d}, \quad (26)$$

$$ADV63_{i,t} = \frac{1}{N_{i,t}} \sum_{d \in \mathcal{W}_t} DVOL_{i,d}, \quad (27)$$

where \mathcal{W}_t is the 63-trading-day window ending at month-end t , and $N_{i,t}$ is the number of days with observed volume in that window. I use monthly cross-sectional liquidity percentiles rather than a fixed dollar-volume cutoff, so the screen adapts to the nominal scale of the market over the long sample.

The selection rule uses hysteresis. An incumbent exits if $CumME_{i,t} > 0.999$ or if its $ADV63$ falls in the bottom 2.5% of that month’s cross-section. A non-constituent enters only if $CumME_{i,t} \leq 0.995$ and its $ADV63$ is at least at the fifth percentile. The stricter entry rule reduces churn near the boundary. For early NASDAQ observations, I defer the liquidity screen until 63 trading days of volume history are available, while still applying the market-cap screen. All screening variables are observed by month-end, and the month-end universe is applied from the first trading day of the next month.

The final universe averages 77.6% of the base common-stock sample while preserving about 99.7% of total market capitalization and 63-day average dollar volume. At the end of 2024, it contains 2,426 of the 3,804 base-sample stocks, with market-cap and dollar-volume preservation rates of 99.78% and 99.28%. The screen therefore removes the extreme illiquid tail while retaining nearly all of the market’s scale.

4.2 Market construction and the aggregate-market gate

The cap-axis bridge is defined relative to an aggregate market return built from the same investable universe. I construct this return, denoted $cMKT$, as a daily value-weighted buy-and-hold portfolio. The month-end universe is held from the first trading day of the next month; weights are based on formation-date market capitalization; returns include dividend-inclusive returns and observable delisting returns; and within-portfolio cash flows are reinvested proportionally across surviving stocks.

The purpose of $cMKT$ is not to reverse-engineer any provider’s market factor. It is the aggregate market return against which every cap-axis bridge is formed. I nevertheless compare it with the Fama–French and q5 market factors to verify that the aggregate benchmark is close to standard provider series. In the common sample, the correlation between $cMKT$ and the Fama–French market return is 0.999778 ($R^2 = 0.999556$), with daily RMSE 2.21 bp and mean absolute error 1.35 bp. Against the q5 market return, the correlation is 0.999799

($R^2 = 0.999598$), with RMSE 2.10 bp and mean absolute error 1.27 bp. The q5 factors used below are the provider’s distributed daily and monthly series, not a frequency conversion of my own. Figure 4.1 shows the daily comparison.

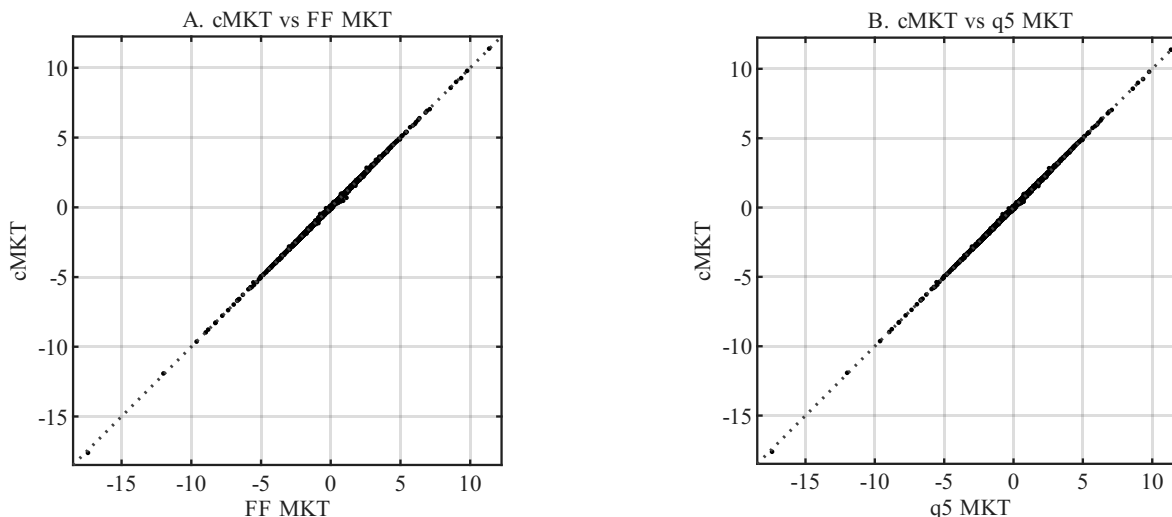


Figure 4.1: CRSP-based market return versus standard market factors

Note: This figure compares the market return $cMKT$, constructed from the CRSP investable universe, with the Fama–French and q5 market returns. The comparison is on a total-market-return basis, with each provider’s risk-free rate added back to the excess market return. The dashed line is the 45-degree line. The common sample runs from January 3, 1967 to December 31, 2024.

I use the aggregate market only as a consistency gate. Since every candidate model contains a market factor, the constructed aggregate market should have a small intercept when used as the test asset. Table 4.1 reports this check. All models have R^2 above 0.999, and all alpha p -values exceed 0.05 under Newey–West standard errors with a 21-trading-day lag.

Table 4.1: Market sanity check on the whole market return

Model	Observations	Annual alpha (bp)	$t(\alpha)$	$p(\alpha)$	R^2
CAPM	14,598	-1.02	-0.22	0.829	0.999556
FF3	14,598	0.21	0.05	0.963	0.999571
Carhart	14,598	-0.06	-0.01	0.989	0.999571
FF5	14,598	-1.07	-0.24	0.812	0.999572
FF6	14,598	-1.18	-0.26	0.792	0.999572
q5	14,598	-5.78	-1.44	0.151	0.999619

Note: This table reports regressions of the whole investable market return on each candidate factor model. Alpha is annualized by multiplying the daily intercept by 252 and is reported in basis points. The sample runs from January 3, 1967 to December 31, 2024. p -values use Newey–West standard errors with a 21-trading-day lag.

Passing this gate does not imply that every portfolio from the same universe has zero alpha. It only rules out the trivial explanation that later bridge results come from failure to price the aggregate benchmark itself. The cap-axis diagnostic asks the conditional question: after the aggregate market is priced, where do pricing errors appear along the capitalization-rank axis?

4.3 Portfolio formation and factor frequency

The main design uses Fama–French-style annual Jul–Jun formation. On the first trading day of each July, stocks in the investable universe are sorted by prior market capitalization. The cap-rank order is then held fixed until the next formation date, and the portfolio is kept buy-and-hold.

Holdings are valued using ex-dividend returns. The difference between dividend-inclusive and ex-dividend returns is pooled as portfolio-level dividend cash and reinvested proportionally across surviving positive-value positions. Bridge and rank-area returns are computed from start-of-day buy-and-hold weights and total returns, so the endpoint condition $D(0) = D(1) = 0$ holds against the market portfolio generated by the same schedule.

I evaluate the same economic cap-axis payoff at two factor frequencies. At the daily frequency, daily bridge returns are regressed on each provider’s daily factors. At the monthly frequency, daily bridge returns are aggregated to calendar months and regressed on each provider’s distributed monthly factors. The market return is compounded within each month,

$$R_{M,m} = \prod_{d \in m} (1 + R_{M,d}) - 1, \quad (28)$$

while zero-investment bridge and rank-area returns are summed:

$$D_m(p) = \sum_{d \in m} D_d(p), \quad (29)$$

$$Y_m = \sum_{d \in m} Y_d. \quad (30)$$

The monthly test is therefore not a smoothed daily regression. It evaluates the same cap-axis payoff at the monthly observation unit using the provider’s monthly factor implementation.

The daily–monthly comparison is reduced-form: it combines observation frequency with factor-frequency implementation. Robustness checks separate this from rebalancing-cycle variation and lead–lag exposure. The main formation cycle is annual Jul–Jun; robustness checks use daily, monthly, quarterly, and annual-Jan formation. Daily formation re-sorts stocks each trading day using prior market capitalization and constructs the bridge from

that day's value-weighted returns. Non-daily formation schemes use the same buy-and-hold dividend-pool accounting as the main design.

4.4 Empirical implementation of the cap-axis diagnostic

The empirical engine implements the finite-asset bridge in [Section 3.4](#). At each grid point, the prefix is formed with whole stocks; the boundary stock is not split. Let $w_{i,t}$ be the start-of-day market weight and $R_{i,t}$ the total return under the relevant formation schedule. For grid point $p_l \in \mathcal{P}$, define

$$k(l, t) = \begin{cases} 0, & p_l = 0, \\ \min \left\{ k : \sum_{i=1}^k w_{i,t} \geq p_l \right\}, & p_l \in (0, 1], \end{cases} \quad s_{l,t} = \sum_{i=1}^{k(l,t)} w_{i,t}. \quad (31)$$

The prefix contribution and bridge return are

$$B_{l,t} = \sum_{i=1}^{k(l,t)} w_{i,t} R_{i,t}, \quad (32)$$

$$D_{l,t} = B_{l,t} - s_{l,t} R_t^M. \quad (33)$$

Thus the bridge longs the realized prefix and shorts the aggregate market at the same realized exposure. Endpoint closure holds by construction.

For each model m , I estimate

$$D_{l,t} = \alpha_m(p_l) + \beta_m(p_l)' f_{m,t} + \varepsilon_{m,l,t}. \quad (34)$$

The baseline grid is uniform on $[0, 1]$ with 201 cutoffs; robustness checks use alternative grids. The compared models are CAPM, FF3, Carhart, FF5, FF6, and q5, all estimated on the common sample shared by the relevant factor series. I also verify that the tail bridge satisfies $D_{l,t} + D_{l,t}^T = 0$ to machine precision.

4.4.1 Rank-area scalar diagnostic

The rank-area portfolio implements the signed area as one zero-investment return. Let

$$m_{i,t} = \sum_{j < i} w_{j,t} + \frac{1}{2} w_{i,t} \quad (35)$$

be stock i 's midpoint cumulative share. Define

$$Y_t = \sum_{i=1}^{N_t} w_{i,t} R_{i,t} \left(\frac{1}{2} - m_{i,t} \right). \quad (36)$$

This portfolio integrates the full bridge path; it is not a size portfolio at one cutoff. Because alpha is linear in the test return, the alpha of Y_t is the scalar counterpart of the signed area when the same sample and factor matrix are used. In finite data, the identity is approximate because the grid bridge uses whole-stock prefixes while Y_t uses midpoint weights. I report the rank-area alpha as the HAC-tested signed-area statistic and verify that the grid-integrated \widehat{SA}_m differs from it by less than 1.5 bp annualized for every model.

4.4.2 Inference: HAC and ordering placebos

Inference has two layers. HAC inference asks whether the signed-area alpha is large relative to time-series uncertainty. Since the rank-area portfolio is a single test return, its alpha is tested with Newey–West standard errors. The main daily lag is 21 trading days, with 5, 63, and 252 trading days used in robustness. The monthly lag is 6 months.

Ordering placebos ask whether the bridge shape is specific to capitalization rank. For each placebo draw, I keep dates, universe, returns, market weights, formation schedule, and split shares fixed, but randomly shuffle only the stock order. I then recompute prefixes, bridge returns, bridge-alpha curves, and functional statistics. In buy-and-hold designs, the random order is drawn once per formation date and held until the next formation date; in daily rebalancing, it is redrawn daily.

The ordering placebo is not a structural null that the factor model is true. It is a matched benchmark for cap-rank specificity. HAC significance indicates time-series evidence for a signed-area alpha. Placebo significance indicates that the curve is unusual relative to random orderings of the same market. I call a result a robust cap-rank distortion only when both layers agree.

For the signed area, the placebo statistic is $|\widehat{SA}|$. For \widehat{IAE} , \widehat{ISE} , and \widehat{SUP} , the placebo statistic is the corresponding upper-tail functional. The factor-coordinate map in [Section 6](#) uses the same bridge construction, with each candidate factor added to the market as a two-factor specification.

5 Empirical Results

This section reports the cap-axis diagnostic under the main annual Jul–Jun formation design. I evaluate the same cap-axis payoff at the daily and monthly factor frequencies. Robustness to alternative rebalancing cycles is reported in [Section 7](#).

5.1 Daily results

The daily sample runs from January 3, 1967 to December 31, 2024, with 14,598 trading days. Each model’s bridge-alpha curve is estimated on a uniform grid of 201 cutoffs. [Table 5.1](#) reports the grid functionals, the rank-area HAC statistic, Rank R^2 , the coherence ratio $|\widehat{SA}|/\widehat{IAE}$, and ordering-placebo tail probabilities.

Table 5.1: Annual Jul–Jun rebalancing, daily frequency: cap-axis bridge functional statistics and inference

Model	\widehat{SA}	t_{NW}	Rank R^2	\widehat{IAE}	\widehat{ISE}	\widehat{SUP}	$\frac{ \widehat{SA} }{\widehat{IAE}}$	$p_{ SA }^{\text{perm}}$	p_{IAE}^{perm}	p_{ISE}^{perm}	p_{SUP}^{perm}
CAPM	−10.9	−0.57	0.003	11.0	186	26.7	0.99	0.119	0.138	0.116	0.143
FF3	21.2	1.94	0.614	21.7	608	42.8	0.97	0.005	0.004	0.003	0.006
Carhart	20.8	1.88	0.614	21.4	587	42.0	0.97	0.001	0.001	0.001	0.002
FF5	7.6	0.71	0.654	10.3	168	29.0	0.74	0.316	0.225	0.194	0.140
FF6	8.2	0.77	0.654	10.5	175	28.3	0.78	0.259	0.187	0.157	0.126
q5	−39.6	−3.49	0.650	39.6	1,910	68.0	1.00	< 0.001	< 0.001	< 0.001	< 0.001

Note: \widehat{SA} , \widehat{IAE} , and \widehat{SUP} are in annualized basis points; \widehat{ISE} is in bp^2 . \widehat{SA} is the grid-integrated signed area. t_{NW} and Rank R^2 are from the rank-area portfolio regression, with Newey–West 21-trading-day standard errors. $|\widehat{SA}|/\widehat{IAE}$ is the coherence ratio measuring directionality conditional on nontrivial magnitude; values near one indicate a mostly one-signed curve. $p_{|SA|}^{\text{perm}}$, p_{IAE}^{perm} , p_{ISE}^{perm} , and p_{SUP}^{perm} are ordering-placebo tail probabilities from 2,500 draws that fix cap weights and randomly shuffle only the stock order. For \widehat{SA} , the placebo statistic is $|\widehat{SA}|$. The entry < 0.001 means none of the 2,500 draws reached the observed value. All results evaluate the annual Jul–Jun rebalancing portfolio on daily factors.

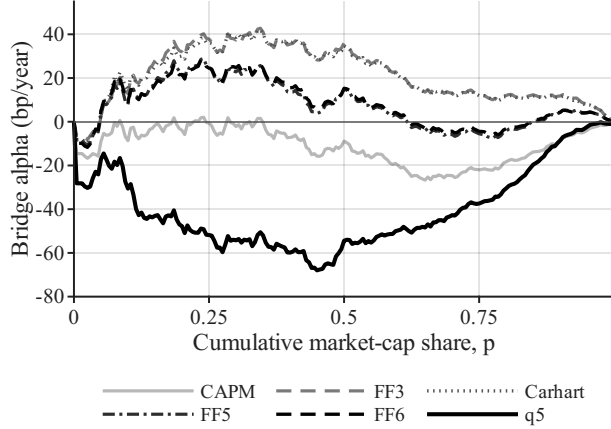


Figure 5.1: Annual Jul–Jun rebalancing, daily frequency: cap-axis bridge-alpha curve
Note: Each candidate model’s estimated bridge-alpha curve $\hat{\alpha}_m(p)$ is plotted against the cumulative market-cap share $p \in [0, 1]$. The vertical axis is in annualized basis points. The q5 curve reaches a minimum of about -68 bp near $p \approx 0.45$, stays in the negative region across the large- to mid-cap range, and closes to zero only at $p = 1$, never changing sign along the cap-axis ($|\widehat{SA}|/\widehat{IAE} = 1.00$). FF3 and Carhart instead form a positive one-signed curve, and FF5 and FF6 change sign near zero. The sample and estimation procedure are as in Table 5.1.

Daily q5 distortion. q5 is the only model with a robust daily cap-axis distortion under both inference layers. Its signed area is -39.6 bp with a rank-area HAC statistic of -3.49 , and all four ordering-placebo probabilities are below the simulation floor. The curve is also almost perfectly directional: $|\widehat{SA}|/\widehat{IAE} = 1.00$, with a local minimum near -68 bp. Thus the daily q5 result is not only large relative to random cap-order assignments, but also statistically visible as a signed-area alpha.

Other daily models. FF5, FF6, and CAPM do not reject cap-axis internal consistency in the main daily design. FF3 and Carhart form a positive bridge with the opposite sign to q5, but their status is weaker: both are unusual under the ordering placebo, while their HAC t -statistics are only borderline. I therefore treat them as cap-order-specific but time-series-weaker daily patterns.

Interpretation. The daily result is axis-restricted. It does not imply that q5 fails to price the aggregate market, which it passes in Table 4.1, nor does it overturn mean–variance comparisons. It shows that, conditional on the aggregate-market gate, q5 leaves a one-sided pricing-error path along the cap-rank axis at the daily factor frequency. The next subsection asks whether this path survives at the monthly frequency.

5.2 Monthly results

I next aggregate the same daily bridge payoffs to calendar months and regress them on the providers' distributed monthly factors. The sample has 696 months. Inference uses a Newey–West 6-month lag and the same ordering-placebo design. Table 5.2 reports the monthly functionals and rank-area statistics.

Table 5.2: Annual Jul–Jun rebalancing, monthly frequency: cap-axis bridge functional statistics and inference

Model	\widehat{SA}	t_{NW}	Rank R^2	\widehat{IAE}	\widehat{ISE}	\widehat{SUP}	$\frac{ \widehat{SA} }{\widehat{IAE}}$	$p_{ SA }^{\text{perm}}$	p_{IAE}^{perm}	p_{ISE}^{perm}	p_{SUP}^{perm}
CAPM	11.6	0.59	0.091	12.3	213	30.0	0.94	< 0.001	< 0.001	< 0.001	< 0.001
FF3	32.4	2.81	0.649	32.5	1,293	57.1	1.00	< 0.001	< 0.001	< 0.001	< 0.001
Carhart	32.8	2.60	0.649	33.0	1,315	57.4	1.00	< 0.001	< 0.001	< 0.001	< 0.001
FF5	32.5	2.87	0.680	32.5	1,293	55.3	1.00	< 0.001	< 0.001	< 0.001	< 0.001
FF6	32.4	2.72	0.680	32.4	1,281	56.4	1.00	< 0.001	< 0.001	< 0.001	< 0.001
q5	4.4	0.40	0.677	5.2	37	13.6	0.83	0.064	0.027	0.026	0.005

Note: Units and definitions are as in Table 5.1. t_{NW} and Rank R^2 are from the monthly rank-area portfolio regression, with Newey–West 6-month standard errors. $p_{|SA|}^{\text{perm}}$, p_{IAE}^{perm} , p_{ISE}^{perm} , and p_{SUP}^{perm} are ordering-placebo tail probabilities. For \widehat{SA} , the placebo statistic is $|\widehat{SA}|$. All results evaluate the annual Jul–Jun rebalancing portfolio after aggregation to monthly returns and assessment on provider monthly factors. At the monthly frequency the ordering placebo has a tight null distribution, so economically small distortions can still appear unusual relative to random cap-order assignments.

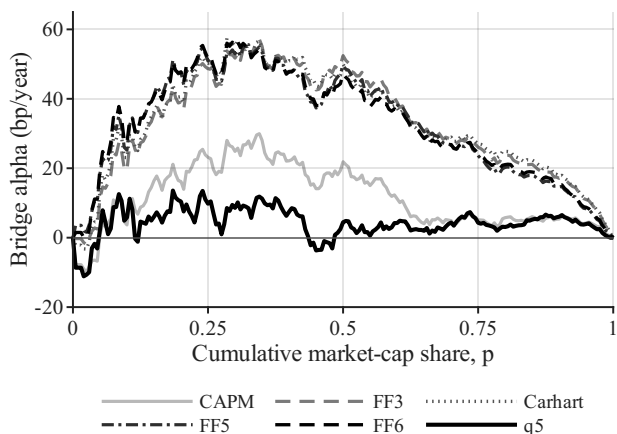


Figure 5.2: Annual Jul–Jun rebalancing, monthly frequency: cap-axis bridge-alpha curve
Note: Same format as Figure 5.1 but at the monthly factor frequency. The FF3, FF5, FF6, and Carhart curves form a positive one-sided bulge reaching a maximum of about +55 to +57 bp near $p \approx 0.33$. The q5 curve stays closer to zero and changes sign, with $|\widehat{SA}|/\widehat{IAE} = 0.83$. The sample and estimation procedure are as in Table 5.2.

Monthly attenuation of q5. At the monthly frequency, q5’s large negative daily signed area is nearly absent. The signed area is +4.4 bp, the HAC statistic is 0.40, and the ordering-placebo probability for $|\widehat{SA}|$ is 0.064. Small local residuals remain in \widehat{IAE} , \widehat{ISE} , and \widehat{SUP} , but the directional daily bridge does not persist.

Monthly Fama–French and Carhart bridge. The Fama–French and Carhart models display the opposite pattern. FF3, Carhart, FF5, and FF6 all have signed areas around +32 bp, coherence ratios near one, HAC statistics between 2.60 and 2.87, and ordering-placebo probabilities below 0.001. The cap-axis distortion that is weak or absent for these models daily becomes visible at the monthly factor frequency.

Frequency interaction. The main empirical message is a frequency-by-model interaction. q5’s cap-axis distortion is concentrated at the daily frequency and attenuates monthly; the Fama–French and Carhart distortions are stronger monthly. This asymmetry matters because daily non-synchronous trading is a natural candidate explanation for daily distortions, but it does not naturally explain a bridge that appears more clearly at the lower monthly frequency. [Section 7.3](#) therefore applies lead–lag corrections to the daily bridge.

The evidentiary status of these two directions is not symmetric. Non-synchronous trading and lead–lag exposure can create daily beta attenuation, so they are natural candidates for a daily distortion. They do not naturally explain a distortion that appears more clearly at the lower monthly frequency. For this reason, the q5 daily bridge requires a lead–lag correction before interpretation, while the monthly positive bridge is less naturally attributed to daily non-synchronous trading. [Section 7.3](#) provides the lead–lag exercise.

In sum, the diagnostic does not produce a single model ranking. It shows where, in what direction, and at which frequency cap-rank pricing errors appear.

6 The Cap-Axis Metric as a Zero-Alpha Factor Coordinate

The preceding sections estimate cap-axis pricing errors at the model level. This section uses the same object as a factor-level coordinate. For each candidate factor, I compare its maximum-Sharpe contribution with the cap-axis footprint left by the two-factor model that adds the factor to the market. This produces a descriptive map of whether Sharpe gain and cap-rank zero-alpha consistency rank factors in the same way. They do not: in the 154-factor universe below, the cap-axis footprint is related to Sharpe gain in the upper tail, but it is not a monotone restatement of either Sharpe improvement or conventional size exposure.

6.1 Construction

For each candidate factor g_j , I estimate a two-factor model containing the market and g_j :

$$D_t(p) = \alpha_j(p) + \beta_{j,M}(p)R_{M,t}^e + \beta_{j,g}(p)g_{j,t} + \varepsilon_{j,t}(p). \quad (37)$$

The factor’s zero-alpha footprint is the bridge-alpha curve $p \mapsto \alpha_j(p)$, summarized by \widehat{SA}_j , \widehat{IAE}_j , \widehat{ISE}_j , and \widehat{SUP}_j . I compare these statistics with the annualized maximum-Sharpe-ratio gain from adding g_j to the market, denoted ΔSR_j .

The candidate set is the monthly factor library of [Jensen et al. \(2023\)](#), accessed through Global Factor Data ([Global Factor Data, 2026](#)), augmented with the Fama–French/Carhart and q5 factors used elsewhere in the paper. After requiring sufficient overlap with the 1967–2024 common sample, the final set contains 154 factors: 144 anomaly-library factors, six Fama–French/Carhart factors, and four q5 nonmarket factors. The cap-axis leg is the annual Jul–Jun bridge summed to months, as in the monthly analysis.

I read the scatter as a descriptive factor map, not as 154 separate hypothesis tests. In this scan, \widehat{IAE} and \widehat{ISE} rank factors almost identically, with Spearman correlation 0.99. I therefore use \widehat{IAE} in the main figure because it is measured in annualized basis points.

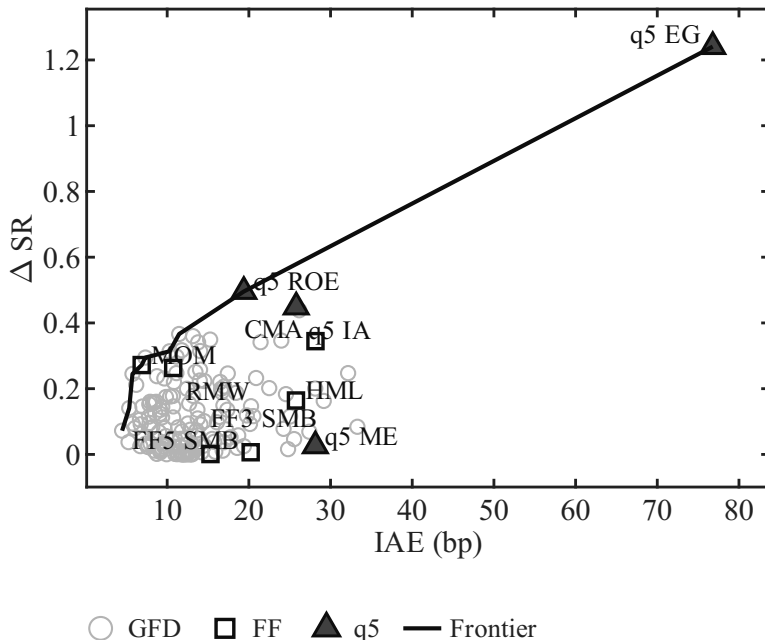


Figure 6.1: Cap-axis footprint versus Sharpe-ratio gain across the factor universe
Note: Each point is one candidate factor added to the market in the 1967–2024 monthly sample. The horizontal axis is the integrated absolute error \widehat{IAE}_j of the cap-axis bridge-alpha curve of the two-factor model $\{R_M^e, g_j\}$, in annualized basis points. The vertical axis is the annualized maximum-Sharpe-ratio gain ΔSR_j from adding g_j to the market. Open circles are Global Factor Data candidates, open squares are Fama–French/Carhart factors, and filled triangles are q5 factors. The solid line traces the upper-left frontier: among candidate factors with no larger cap-axis footprint, it records the largest observed Sharpe-ratio gain.

6.2 Sharpe gain and zero-alpha footprint

Figure 6.1 shows that the cap-axis footprint and the Sharpe coordinate order factors differently. Across the 154 factors, the rank correlation between ΔSR and \widehat{IAE} is only 0.15. The linear correlation is higher, 0.54, because the upper-right tail contains factors with both large Sharpe gains and large cap-axis footprints. q5 expected growth is the clearest case: it has the largest Sharpe gain, $\Delta SR = 1.24$, and the largest footprint, $\widehat{IAE} = 76.8$ bp.

The high-Sharpe, low-footprint region is also populated: thirty-four factors sit above the median Sharpe gain while below the median cap-axis footprint. I therefore do not interpret the scatter as a universal tradeoff. The narrower point is that the two coordinates are distinct. ΔSR_j measures what a factor adds to the attainable frontier; \widehat{IAE}_j measures the pricing-error curve left on a fixed market-internal subspace when the same factor is added to the market.

6.3 The footprint is not size exposure

Because the axis is ordered by market capitalization, a natural concern is that the cap-axis footprint merely relabels size exposure. I test this using q5 ME as a traded size proxy. For every candidate factor g_j , I estimate

$$g_{j,t} = a_j + b_{j,M}R_{M,t}^e + \gamma_{j,size}ME_t^{q5} + u_{j,t}, \quad (38)$$

and ask whether $|\widehat{\gamma}_{j,size}|$ explains the cross-section of cap-axis footprints.

It does not. Regressing \widehat{IAE} on the absolute size loading gives $R^2 = 0.000137$, and the rank correlation between $|\widehat{\gamma}_{size}|$ and \widehat{IAE} is -0.03 . The same pattern holds for the other magnitude norms: the size-loading R^2 is 0.000004 for \widehat{ISE} , 0.005199 for \widehat{SUP} , and 0.005546 for $|\widehat{SA}|$. Residualizing the norms with respect to size exposure leaves their rank relation with ΔSR essentially unchanged.

Table 6.1: Size-controlled nonreducibility of the cap-axis footprint

Norm	Pearson with ΔSR	Spearman with ΔSR	High-high count	Size-loading R^2	Size-resid. Spearman
\widehat{ISE}	0.650	0.145	35	0.000004	0.153
\widehat{IAE}	0.543	0.149	34	0.000137	0.161
\widehat{SUP}	0.460	0.069	38	0.005199	0.073
$ \widehat{SA} $	0.478	0.076	37	0.005546	0.081

Note: The table reports the 154-factor monthly scan. High-high count denotes factors above both the median ΔSR and the median reported norm. Size-loading R^2 is the cross-sectional explanatory power of the absolute size loading $|\widehat{\gamma}_{j,size}|$ from Equation (38). Size-resid. Spearman is the Spearman correlation between ΔSR and the size-residualized norm. The magnitude norms are not explained by conventional size-factor exposure. The signed area itself is different: $\text{Spearman}(\widehat{SA}, \widehat{\gamma}_{size}) = 0.65$, because \widehat{SA} preserves directional tilt along the cap-axis.

Table 6.1 summarizes the audit. The cap-axis diagnostic is size-ordered by construction, but its magnitude norms are not explained by conventional size-factor loading. A traded size factor can load strongly on the market-cap dimension without producing the largest cap-axis footprint, and a factor with modest size loading can still leave a large bridge-alpha curve.

Table 6.2 gives the same point at the factor level. q5 expected growth has the largest footprint, $\widehat{IAE} = 76.8$ bp, but its market-controlled loading on q5 ME is only -0.21 . The Fama-French SMB factors provide the opposite comparison: they load 0.93–0.97 on q5 ME, but their cap-axis footprints are smaller and their Sharpe gains are close to zero.

Table 6.2: Cap-axis footprint, Sharpe gain, and size loading: selected extremes

Factor	Family	ΔSR	\widehat{IAE} (bp)	size β
<i>Panel A. Largest cap-axis footprints</i>				
q5 EG	q5	1.24	76.8	-0.21
corr 1260d	GFD	0.08	33.3	0.47
seas 6-10na	GFD	0.25	32.1	0.09
ncoa gr1a	GFD	0.16	29.2	0.23
CMA	FF	0.34	28.2	0.04
q5 ME	q5	0.03	28.1	-
nncoa gr1a	GFD	0.20	28.1	0.18
sale me	GFD	0.07	27.4	0.30
<i>Panel B. Smallest cap-axis footprints</i>				
gp at	GFD	0.07	4.5	-0.14
op at11	GFD	0.04	5.3	-0.25
seas 11-15an	GFD	0.14	5.4	-0.06
seas 6-10an	GFD	0.24	5.8	0.01
op at	GFD	0.09	5.8	-0.27
niq at	GFD	0.08	6.0	-0.33
<i>Memo: size factors</i>				
FF3 SMB	FF	0.00	15.3	0.93
FF5 SMB	FF	0.01	20.2	0.97

Note: ΔSR is the annualized maximum-Sharpe-ratio gain from adding the factor to the market. \widehat{IAE} is the integrated absolute error of the cap-axis bridge-alpha curve of $\{R_M^c, g_j\}$, in annualized basis points. Size β is the factor's market-controlled loading on q5 ME from Equation (38); it is omitted for q5 ME because q5 ME is the benchmark size proxy. Factors are sorted within panels by \widehat{IAE} .

The size-nonreducibility claim concerns curve magnitude and shape, not signed direction. The signed area is different by design: because \widehat{SA} preserves directional tilt along the cap-axis, it naturally correlates with signed size tilt; in the scan, $\text{Spearman}(\widehat{SA}, \widehat{\gamma}_{size}) = 0.65$. Thus \widehat{SA} captures direction, while \widehat{IAE} , \widehat{ISE} , and \widehat{SUP} capture magnitude.

6.4 Model-level cancellation in factor space

The factor-coordinate map also illustrates model-level cancellation. At the monthly frequency, the full q5 model has a small cap-axis footprint in Table 5.2: $\widehat{IAE} = 5.2$ bp and $\widehat{ISE} = 37$. Yet several q5 constituent factors have large marginal footprints when added to the market one at a time. Expected growth is the largest observed footprint, and investment, size, and profitability also have visible footprints relative to the market-only benchmark.

This does not decompose the full q5 model. The scan measures each factor’s marginal cap-axis footprint when added to the market, not its contribution inside the assembled q5 specification. It shows only that model-level consistency need not come from cap-axis-neutral components. A factor model can combine factors with large marginal zero-alpha footprints and still produce a small assembled bridge-alpha curve through offsetting exposures.

7 Robustness

This section checks whether the frequency-by-model patterns are artifacts of implementation choices. The checks have distinct roles. Ordering placebos benchmark cap-rank specificity. Rebalancing checks test dependence on the formation cycle. Lead-lag corrections ask whether daily bridge alphas, especially q5’s negative signed area, are absorbed by short-horizon beta attenuation.

7.1 Ordering-placebo distributions

The ordering placebo fixes dates, universe, market weights, and returns, and randomizes only the stock order. It is not a structural null that the factor model is true. It is a matched benchmark for cap-rank specificity: a small placebo tail probability means that the observed bridge statistic is difficult to reproduce after destroying the capitalization ordering.

[Table 7.1](#) reports the daily signed-area placebo. The null distribution is centered near zero with a standard deviation of about 7 bp. q5’s observed signed area lies far outside this distribution. FF3 and Carhart also exceed the upper tail, while CAPM, FF5, and FF6 remain inside the placebo range.

Table 7.1: Ordering-placebo null distribution versus observed: daily frequency

Model	Observed	Null mean	Null SD	Null p_5	Null p_{95}	$p_{ SA }^{\text{perm}}$
CAPM	-10.6	-0.0	6.8	-11.2	10.9	0.117
FF3	20.8	0.0	7.3	-11.5	12.2	0.006
Carhart	20.6	-0.0	6.6	-10.5	10.9	0.002
FF5	7.4	0.0	7.5	-12.4	12.4	0.316
FF6	8.2	-0.0	7.1	-11.6	11.6	0.248
q5	-38.3	-0.1	7.4	-12.0	12.3	< 0.001

Note: Both observed values and placebo values are rank-area signed areas, annualized in basis points. The placebo distribution is obtained from 2,500 draws that fix cap weights and returns and randomly shuffle only the stock order. The table reports the placebo mean, standard deviation, and 5th and 95th percentiles. $p_{|SA|}^{\text{perm}}$ is the ordering-placebo tail probability for $|\widehat{SA}|$. The entry < 0.001 means that no draw reached the observed value. The sample is daily, annual Jul–Jun rebalancing, 1967–2024.

Table 7.2 reports the monthly signed-area placebo. The null distribution is much tighter, with standard deviations around 2 bp. The positive monthly signed areas of FF3, Carhart, FF5, and FF6 are extreme under this benchmark. CAPM is also extreme under the placebo, but its HAC statistic in Table 5.2 is weak, so I treat it as a placebo-only cap-order pattern. q5’s monthly signed area is small and not rejected at conventional levels by the signed-area placebo.

Table 7.2: Ordering-placebo null distribution versus observed: monthly frequency

Model	Observed	Null mean	Null SD	Null p_5	Null p_{95}	$p_{ SA }^{\text{perm}}$
CAPM	11.6	-0.3	2.0	-3.6	3.0	< 0.001
FF3	32.4	-0.3	2.0	-3.7	3.0	< 0.001
Carhart	32.8	-0.4	2.0	-3.7	3.0	< 0.001
FF5	32.5	-0.4	2.0	-3.7	3.0	< 0.001
FF6	32.4	-0.4	2.0	-3.7	3.0	< 0.001
q5	4.4	-0.3	2.3	-4.2	3.5	0.064

Note: Both observed values and placebo values are rank-area signed areas, annualized in basis points, measured at the monthly factor frequency. The portfolio is annual Jul–Jun rebalancing, with daily bridge returns summed to calendar months and regressed on provider monthly factors. The placebo distribution is obtained from 2,500 draws that fix cap weights and returns and randomly shuffle only the stock order. $p_{|SA|}^{\text{perm}}$ is the ordering-placebo tail probability for $|\widehat{SA}|$. The entry < 0.001 means that no draw reached the observed value.

The signed-area placebo reinforces the frequency-by-model pattern without replacing HAC inference. q5 has a large negative daily signed area but a small monthly signed area.

The Fama–French-family and Carhart models have the opposite pattern: their positive bridge is weaker daily and much larger monthly. q5 is not exactly residual-free monthly, because its local curve measures remain unusual in [Table 5.2](#); the precise claim is that its directional signed area attenuates sharply.

7.2 Dependence on the rebalancing cycle

The main design uses annual Jul–Jun formation. I vary the formation cycle to daily, monthly, quarterly, and annual-Jan schedules. The goal is not to search for the strongest rejection, but to check whether the frequency pattern depends on one rebalancing convention.

The pattern is stable. Under daily factor evaluation, q5 has the most negative signed area across formation cycles, while FF5 and FF6 remain closer to zero. Under monthly factor evaluation, FF3, Carhart, FF5, and FF6 display positive bridges, while q5 remains close to zero. The daily–monthly reversal is therefore not an artifact of annual Jul–Jun formation.

[Figure 7.1](#) shows the result for q5 and FF5. q5 curves are negative at the daily factor frequency and close to zero monthly. FF5 is small daily and positive monthly. The vertical-axis range differs across panels, so the figure should be read for shape and sign rather than exact cross-panel magnitudes.

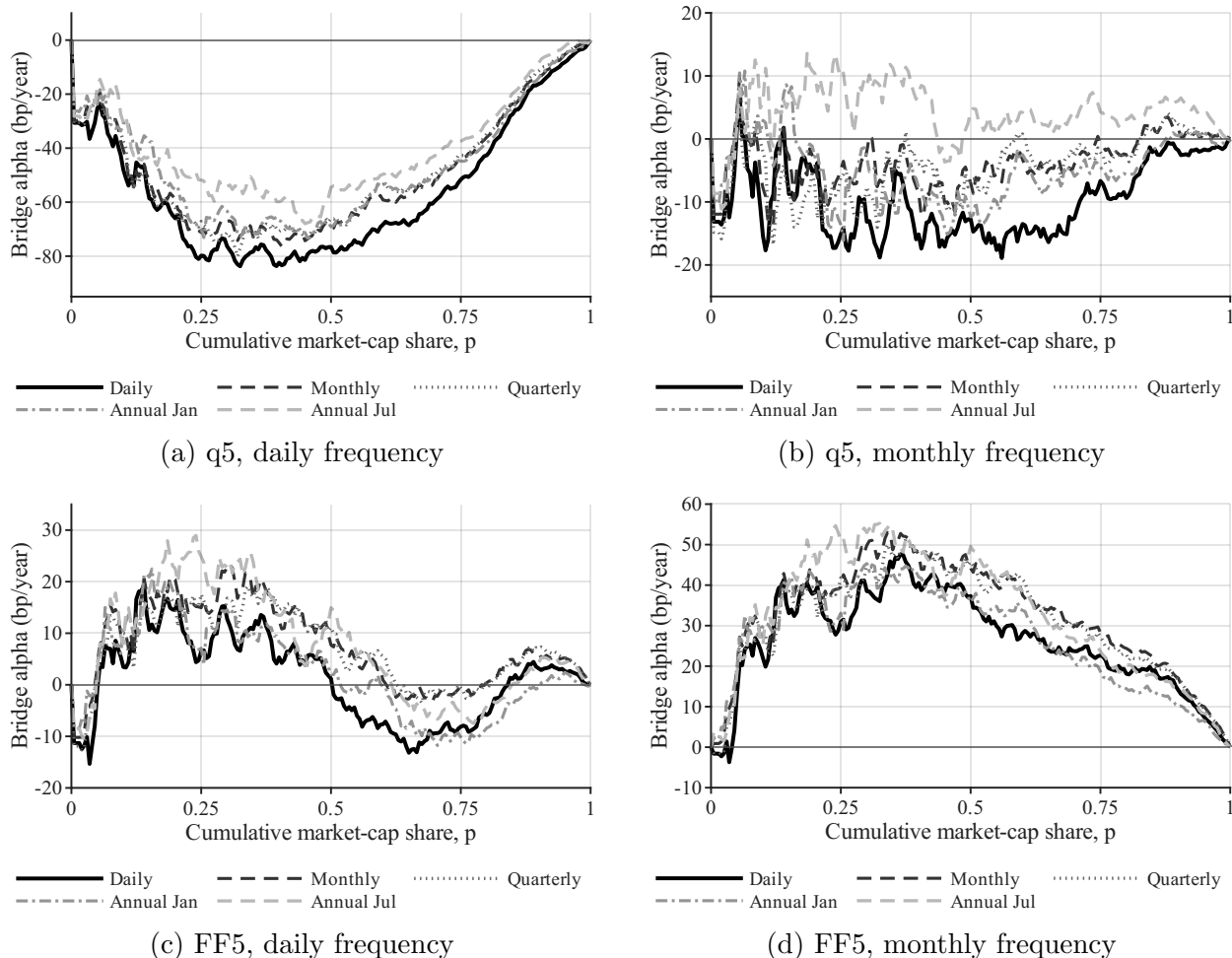


Figure 7.1: Cap-axis bridge-alpha curves by formation cycle

Note: Each panel plots the bridge-alpha curve, annualized in basis points, against cumulative market-cap share $p \in [0, 1]$, overlaying five formation cycles: daily, monthly, quarterly, annual Jan, and annual Jul. The top row is q5 and the bottom row is FF5. The left column uses daily factors and the right column uses monthly factors. The vertical-axis range differs across panels.

Magnitude varies with formation frequency. For q5 under daily factor evaluation, the negative signed area grows as the formation cycle shortens, from -39.6 bp under annual Jul–Jun formation to -55.2 bp under daily formation. This is consistent with a high-frequency component amplified when the cap-rank order and small-stock boundary are updated more often. Alternative grids and HAC lags do not change the ranking of the main functionals.

7.3 Non-synchronous trading and the lead–lag correction

The daily q5 bridge is the result most exposed to a non-synchronous-trading interpretation. If small or illiquid stocks react to factors with a lag, daily betas can be attenuated and bridge alphas can appear. I therefore apply a Dimson-style lead–lag correction, closely related to

the Scholes–Williams adjustment.

For each model, I augment the bridge regression with factor leads and lags over a symmetric window $[-k, +k]$. The corrected exposure is the sum of coefficients across the window, and the corrected alpha is the intercept of the extended regression. I report $k \in \{1, 2, 3, 5, 8, 10, 13, 21\}$. The naive estimate is recomputed on each k -trimmed sample, so changes across columns reflect the correction rather than sample dropout.

Table 7.3 reports the horizon profile for the main annual Jul–Jun bridge. The table should be read as a frequency gate, not as a single pass/fail test.

Table 7.3: Horizon profile of the lead–lag-corrected rank-area signed area (annual Jul–Jun rebalancing, ann bp)

Model	Naive	$k=1$	$k=2$	$k=3$	$k=5$	$k=8$	$k=10$	$k=13$	$k=21$
CAPM	−10	1	5	8	13	15	15	17	20
FF3	21	27*	27*	27*	27*	26*	26*	25*	22*
Carhart	21	28*	27*	27*	27*	24*	24*	24*	21
FF5	7	18	20*	20	19	23*	26*	28*	28*
FF6	8	19	21*	20	20	22*	24*	27*	26*
q5	−38***	−23*	−15	−14	−9	−6	−6	−1	6

Note: Each cell is the lead–lag-corrected rank-area signed area, annualized in basis points and rounded to integers. The Naive column is the uncorrected estimate on the same trimmed sample. *, **, and *** denote 5%, 1%, and 0.1% significance by the Newey–West 21-trading-day t -statistic. k is the one-sided number of trading days in the symmetric lead–lag window. The sample is annual Jul–Jun rebalancing, 1967–2024 common sample, with 14,556–14,596 trading days depending on the per- k trim.

The q5 signed area attenuates rapidly. The naive estimate is −38 bp and strongly significant. With one lead and lag it falls to −23 bp; from $k = 2$ onward it is no longer significant; by $k = 21$, it is +6 bp. Most attenuation therefore occurs within the first few leads and lags, where a non-synchronous-trading interpretation is most plausible.

The other models have different profiles. FF3 remains positive and significant through $k = 21$, Carhart remains significant through $k = 13$, and FF5 and FF6 become positive at wider windows. The correction therefore does not mechanically shrink every bridge toward zero. It specifically absorbs the negative daily q5 signed area while leaving the Fama–French-family positive bridge intact or stronger.

A daily-rebalancing worst-case check. Daily formation re-sorts the cap-axis order every trading day and updates the small-stock boundary most frequently. It is therefore a

worst-case design for non-synchronous-trading exposure. I apply the same lead-lag correction to the daily-rebalancing bridge in [Table 7.4](#).

Table 7.4: Horizon profile of the lead-lag-corrected rank-area signed area (daily rebalancing, ann bp)

Model	Naive	$k=1$	$k=2$	$k=3$	$k=5$	$k=8$	$k=10$	$k=13$	$k=21$
CAPM	-13	-2	2	6	11	13	14	16	17
FF3	18	25*	25*	25*	25*	24*	24*	22*	19
Carhart	9	15	16	16	16	13	13	12	9
FF5	1	11	13	14	12	18	21	24*	24*
FF6	-5	4	7	7	6	9	12	14	13
q5	-54***	-41***	-33**	-30**	-25*	-17	-17	-11	-3

Note: Each cell is the lead-lag-corrected rank-area signed area, annualized in basis points and rounded to integers. The Naive column is the uncorrected estimate on the same trimmed sample. *, **, and *** denote 5%, 1%, and 0.1% significance by the Newey–West 21-trading-day t -statistic. k is the one-sided number of trading days in the symmetric lead-lag window. $k = 21$ is about one trading month. The sample is daily rebalancing, 1967–2024 common sample.

The daily-rebalancing profile moves in the same direction but starts from a larger negative value. q5’s naive signed area is -54 bp, remains significant through $k = 5$, becomes insignificant at wider windows, and reaches -3 bp by $k = 21$. This is the expected pattern in the worst-case design: the distortion is stronger when the cap-rank boundary is updated daily, but it still disappears over a one-month lead-lag window.

Together, the lead-lag exercises localize the daily q5 bridge in a short-horizon window. The same correction does not absorb the Fama–French-family positive bridge, which appears more clearly at the monthly frequency. The robustness evidence therefore supports the paper’s main interpretation: the diagnostic measures where along the cap-rank axis, and at which horizon, each model leaves pricing error.

8 High-Resolution Zero-Alpha Diagnostics versus Size-Bin Tests

The cap-axis diagnostic is not a replacement for size-sorted portfolio tests. It answers a different zero-alpha question on the same economic coordinate. A size-bin test asks whether a finite set of prechosen portfolios has nonzero alphas. The cap-axis diagnostic asks where pricing errors appear as the market portfolio is traversed by cumulative capitalization rank.

The distinction is resolution. A bin test assigns one alpha to each portfolio and therefore compresses any within-bin structure. The cap-axis diagnostic estimates the function $p \mapsto \alpha_m(p)$, where p is cumulative market-capitalization share, and summarizes the path by signed and unsigned integral statistics. This makes prefixes, tails, intervals, and step-function combinations observable on a common coordinate rather than hidden inside a finite partition.

This matters because size bins inherit the aggregation problem that motivates the paper. A model can price the aggregate market while body and tail errors offset inside it. A size-bin test reduces the scale of aggregation, but does not eliminate it: each bin can still average over internal pricing-error structure. The cap-axis curve treats resolution as a grid choice and localizes the error along the market's own capitalization axis.

8.1 Market value concentration inside size bins

The loss of resolution is especially severe for NYSE-breakpoint size deciles because market value is concentrated in the largest bin. [Table 8.1](#) reports the average share of aggregate investable market capitalization held by each size decile from 1967 to 2024. The top decile holds 60.3% of market value on average, with a median of 60.7% and a maximum of 76.4%. The top two deciles together hold 73.7%, and the top three hold 81.4%. Thus most of the market's economic weight is represented by only a few bin-level alphas.

The dominant bin is also internally concentrated. Although the top decile contains 160 stocks on average, its effective number of constituents, measured by the inverse Herfindahl of within-decile weights, is only about 65. Its five largest firms alone account for 20.3% of the entire market. The top decile is therefore not a homogeneous large-stock block, but a steeply cap-weighted submarket with its own internal capitalization-rank structure.

Table 8.1: Concentration of market value across NYSE-breakpoint size deciles

Decile	Mean cap-share	Median	Max	Mean # stocks	Effective #
D01 (small)	1.6%	1.6%	3.8%	1,938	1,328
D02	1.5%	1.5%	2.8%	586	563
D03	1.8%	1.7%	3.1%	389	381
D04	2.2%	2.2%	3.7%	307	302
D05	2.8%	2.7%	4.6%	254	250
D06	3.6%	3.5%	5.4%	214	211
D07	5.0%	5.0%	7.2%	194	190
D08	7.7%	7.9%	10.0%	179	174
D09	13.4%	13.6%	15.8%	166	158
D10 (large)	60.3%	60.7%	76.4%	160	65

Note: Each row reports the time-series average, over the 696 months from January 1967 to December 2024, of one NYSE-breakpoint size decile’s share of aggregate investable market capitalization. Breakpoints are computed from NYSE common stocks and applied to the full investable universe. “Effective #” is the inverse Herfindahl of within-decile capitalization weights. The top decile alone holds a median 60.7% of market value and has an effective constituent count of about 65 despite an average of 160 member stocks.

8.2 Resolution as a zero-alpha functional

The cap-axis diagnostic removes the bin ceiling by making resolution a grid choice. The baseline grid has 201 cutoffs, stepping through the market in half-percentage-point increments of cumulative market value. Because the coordinate starts from the largest stocks, the top NYSE size decile occupies the front of the axis, from $p = 0$ to about $p = 0.60$. A decile test represents this entire region by one alpha. The baseline cap-axis curve resolves the same region with more than one hundred bridge alphas.

The gain is not merely visual. The object being estimated is a zero-alpha function, $p \mapsto \alpha_m(p)$. The functional summaries \widehat{SA} , \widehat{IAE} , \widehat{ISE} , and \widehat{SUP} use the whole path. A bin test can detect that a model has difficulty with a size-sorted portfolio. The cap-axis diagnostic shows whether the error is one-sided or oscillatory, whether it is concentrated near the largest firms or the middle of the dominant bin, and whether it cancels inside a coarser portfolio.

The main results illustrate this difference. In the daily q5 case, the bridge reaches its deepest point near $p \approx 0.45$, well inside the top-decile block. In the monthly Fama–French case, the positive bridge peaks near $p \approx 0.33$, again inside the same economically dominant region. These are not separate decile-level facts. They are within-bin locations on a cumulative-capitalization coordinate.

8.3 Inside the dominant bin: deciles versus the curve

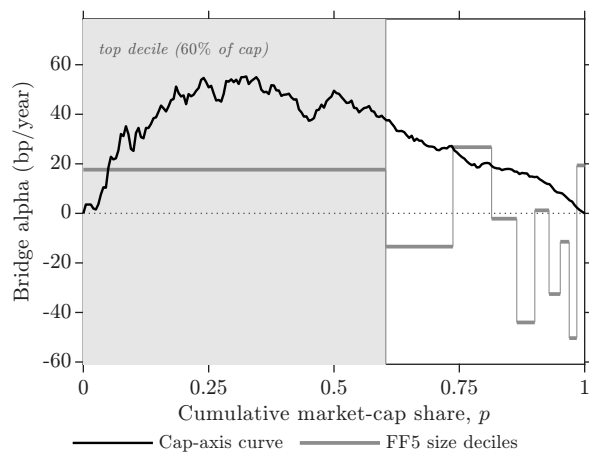


Figure 8.1: The size-decile test collapses the dominant bin into one alpha; the cap-axis curve resolves its interior

Note: Both objects use the Fama–French five-factor model on the common 1967–2024 monthly sample. The black line is the cap-axis bridge-alpha curve $\hat{\alpha}(p)$ under the main annual July design. The gray step plots the ten NYSE-breakpoint size-decile alphas, each spanning the cap-share interval its decile occupies on the cumulative-capitalization axis. Because the axis accumulates value from the largest stocks first, the top decile occupies the front of the axis. The shaded region marks that top decile, which holds a mean 60.3% of aggregate market value and is represented by a single alpha of +17.6 bp, while the continuous curve reaches +55.3 bp near $p \approx 0.33$ inside the same region. Decile alphas are Newey–West 6-month intercepts; none of the ten is significant at conventional levels.

Figure 8.1 overlays the two objects on the same cumulative-capitalization axis. The gray step function is the Fama–French five-factor alpha of each NYSE-breakpoint size decile, drawn over the cap-share interval occupied by that decile. The black line is the monthly cap-axis bridge-alpha curve. Both are estimated on the common 1967–2024 monthly sample.

The contrast is sharp inside the top decile. The decile test assigns the entire shaded region one alpha, +17.6 bp annualized. The cap-axis curve is not flat over that region. It rises from the large-cap endpoint to about +55.3 bp near $p \approx 0.33$, then declines. Thus the largest local bridge alpha inside the top decile is more than three times the bin alpha assigned to the whole region.

The lower deciles show the opposite problem. Their alphas vary across bins, but the bins occupy narrow market-cap intervals and are economically thin. The decile test spends most of its test assets on the small-cap end, where estimates are noisy, while compressing most market value into one large-cap alpha. The cap-axis diagnostic reverses this allocation: it uses uniform resolution in market-value space and therefore devotes more effective resolution to the economically dominant part of the market.

The methodological gain is localization, not simply rejection. A size-decile test may already reject a model in some settings. The cap-axis diagnostic adds where the error is, how it is shaped, and whether it is hidden by within-bin averaging. It turns a finite-bin alpha table into a high-resolution zero-alpha diagnostic on the market’s own capitalization axis.

9 Discussion

What the diagnostic identifies. The cap-axis diagnostic identifies an intermediate object. It does not test whether a candidate SDF prices the entire asset space, and it is not merely a test on a finite list of size portfolios. [Proposition 1](#) gives the restricted object: pricing consistency on the subspace \mathcal{V}_{cap} generated by the aggregate market and the cap-axis bridges.

The bridge-alpha curve measures how pricing error is distributed inside the market portfolio along capitalization rank. A model can price the aggregate market while leaving offsetting errors across prefixes and tails. The bridge unpacks this cancellation cutoff by cutoff. A nonzero curve therefore means that, conditional on the aggregate-market gate, pricing error remains on the restricted cap-rank subspace. The signed area records direction; *IAE*, *ISE*, and *SUP* record magnitude and local distortion; and the coherence ratio records whether the curve is mostly one-signed or oscillatory. The object is best read as a geometry of cap-rank pricing error, not as a binary verdict.

Relation to standard criteria. The diagnostic is complementary to joint alpha tests, Hansen–Jagannathan distance, spanning tests, maximum–Sharpe comparisons, and size-portfolio tests. These tools evaluate pricing errors or mean–variance performance in their own spaces. The cap-axis diagnostic fixes one market-internal coordinate, lifts pricing error into a function on that coordinate, and summarizes the function by directional and global norms.

This distinction matters for low-dimensional factor approximations. A factor span can improve the attainable mean–variance frontier while leaving nonzero alphas on a fixed internal subspace. Conversely, a model can have a small cap-axis footprint without being the strongest mean–variance model. The diagnostic is therefore not an alternative to maximum–Sharpe model comparison. It asks a different question: whether a factor span that is useful for the frontier also satisfies zero-alpha consistency on the cap-rank bridge family.

[Section 8](#) gives the same point relative to size-bin tests. A size-bin test can detect zero-alpha violations on a finite partition, but it averages away structure inside each bin. The cap-

axis diagnostic estimates the zero-alpha path along cumulative market value. Its contribution is localization: it shows where along the capitalization axis the error is concentrated and whether it is hidden by coarser aggregation.

Frequency and horizon dependence. The empirical results show that cap-rank pricing errors are horizon dependent. q5 has a large negative signed area at the daily factor frequency, but this directional bridge attenuates sharply at the monthly frequency. The lead-lag correction gives the same message: as factor leads and lags are added, q5's daily signed area moves toward zero. This pattern is consistent with a short-horizon cap-rank imbalance, plausibly related to non-synchronous trading or factor-frequency mismatch, rather than an unconditional failure of the q5 model.

The Fama-French-family and Carhart models show the opposite horizon profile. Their positive bridges are weaker or borderline daily and become more visible monthly. The lead-lag correction does not absorb these positive bridges in the same way. Thus the diagnostic does not produce a single model ranking. It shows that different models place their cap-rank pricing errors at different horizons.

The factor-coordinate interpretation. The factor-coordinate exercise in [Section 6](#) gives a cross-sectional version of the same idea. Across 154 factors, the cap-axis footprint is not a monotone restatement of maximum-Sharpe gain. A factor can add substantially to the mean-variance frontier and still leave a large zero-alpha footprint on the cap-rank bridge space. Nor is the magnitude of that footprint explained by conventional size-factor loading. The diagnostic is size-ordered by construction, but its integral norms measure the size and shape of a pricing-error curve, not merely exposure to a traded size factor.

This makes the cap-axis norm useful as a factor coordinate. ΔSR measures what a factor adds to the attainable frontier. \widehat{IAE} , \widehat{ISE} , and \widehat{SUP} measure how much pricing-error curve remains on a fixed internal subspace when the same factor is added to the market. The two coordinates can overlap in the upper tail, as with q5 expected growth, but they do not rank factors in the same way.

Potential as a functional object. The bridge-alpha curve is a function, not only a test statistic. This makes it usable beyond the applications in this paper. The integral norms could serve as objective functions for factor construction or model selection, choosing combinations that minimize cap-rank pricing error. Differences between curves could be used to study which factor block moves which cap-rank segment. These operations are feasible in finite data because the curve is already estimated on a grid. I leave minimum-*ISE* factor

construction and factor-block decomposition to future work.

Limitations. The diagnostic is deliberately restricted. Passing it means pricing consistency on the cap-rank subspace, not full SDF validity. Errors along momentum, value, profitability, investment, industry, and idiosyncratic long–short directions may remain outside the test. Conversely, failing the diagnostic means only that the model leaves pricing error on this internal axis. It does not imply that the model lacks mean–variance value or fails in other asset spaces.

The monthly q5 result illustrates the required caution. Its directional signed-area distortion nearly disappears relative to the daily result, but small local residuals remain in *IAE*, *ISE*, and *SUP*. This is neither a clean exoneration nor a broad rejection. More generally, the findings should be read as a map of direction, magnitude, location, and horizon of cap-rank pricing error. The contribution is the measurement device: it shows that aggregate-market fit, maximum-Sharpe improvement, and restricted zero-alpha consistency on the cap-rank subspace are distinct empirical criteria for low-dimensional factor models.

10 Conclusion

This paper defines a cap-axis integral diagnostic for factor-model evaluation. The diagnostic decomposes the market portfolio by cumulative market-capitalization rank and pairs each prefix with an equal-exposure aggregate-market short leg. The resulting bridge-alpha curve is closed at both endpoints and measures how pricing error is distributed inside the market portfolio. Under an aggregate-market consistency gate, a zero bridge-alpha curve is equivalent to pricing the restricted cap-rank subspace generated by the market and the cap-axis bridges.

Applied to the 1967–2024 CRSP market, the diagnostic reveals pricing-error patterns that are not visible from the aggregate market alone. q5 has a one-sided negative bridge at the daily frequency, but this signed-area distortion attenuates under lead–lag correction and is nearly absent monthly. The Fama–French-family and Carhart models show the opposite horizon profile: their bridges are weaker daily but become positive and one-signed monthly. The result is not a model ranking. It shows that cap-rank pricing errors are model-specific and horizon-localized.

The diagnostic also defines a factor-level coordinate. Across 154 monthly factors, the cap-axis footprint is not a monotone restatement of maximum-Sharpe gain and is not mechanically explained by loading on a benchmark size factor. Aggregate-market fit, maximum-Sharpe improvement, size exposure, and restricted cap-rank zero-alpha consistency are there-

fore distinct empirical dimensions.

The interpretation is deliberately restricted. Passing the diagnostic does not imply full SDF validity, and failing it does not imply that a model lacks mean–variance value or fails in other asset spaces. The diagnostic says something narrower: conditional on pricing the aggregate market, does the model leave systematic pricing error along the market’s internal cap-rank axis?

Because the bridge-alpha curve is a function rather than only a test statistic, it can be used beyond the present application. Future work can use *IAE* or *ISE* as objectives for factor construction, impose cap-axis consistency as a model-selection constraint, or decompose the curve to identify which factor blocks move which cap-rank segments. This paper contributes the measurement device and shows that restricted zero-alpha structure can be hidden by aggregate-market tests, maximum-Sharpe summaries, and coarse size-bin comparisons.

Funding This research did not receive any specific grant from funding agencies in the public, commercial, or not-for-profit sectors.

Declaration of AI usage During the preparation of this manuscript, the author used ChatGPT (OpenAI) and Claude (Anthropic) for language refinement and structural clarity. All outputs were reviewed and edited by the author, who takes full responsibility for the content.

Declaration of interest The author declares no competing interests.

References

- Scholes, M., & Williams, J. (1977). Estimating betas from nonsynchronous data. *Journal of Financial Economics*, 5(3), 309–327. [https://doi.org/10.1016/0304-405X\(77\)90041-1](https://doi.org/10.1016/0304-405X(77)90041-1)
- Dimson, E. (1979). Risk measurement when shares are subject to infrequent trading. *Journal of Financial Economics*, 7(2), 197–226. [https://doi.org/10.1016/0304-405X\(79\)90013-8](https://doi.org/10.1016/0304-405X(79)90013-8)
- Gibbons, M. R., Ross, S. A., & Shanken, J. (1989). A test of the efficiency of a given portfolio. *Econometrica*, 57(5), 1121–1152. <https://www.jstor.org/stable/1913625>
- Lo, A. W., & MacKinlay, A. C. (1990). Data-snooping biases in tests of financial asset pricing models. *The Review of Financial Studies*, 3(3), 431–467. <https://doi.org/10.1093/rfs/3.3.431>
- Hansen, L. P., & Jagannathan, R. (1997). Assessing specification errors in stochastic discount factor models. *The Journal of Finance*, 52(2), 557–590. <https://doi.org/10.1111/j.1540-6261.1997.tb04813.x>
- Cochrane, J. H. (2005). *Asset Pricing* (Revised ed.). Princeton University Press. <https://www.johnhcochrane.com/asset-pricing>
- Lewellen, J., Nagel, S., & Shanken, J. (2010). A skeptical appraisal of asset-pricing tests. *Journal of Financial Economics*, 96(2), 175–194. <https://doi.org/10.1016/j.jfineco.2009.09.001>
- Barillas, F., & Shanken, J. (2017). Which alpha? *The Review of Financial Studies*, 30(4), 1316–1338. <https://doi.org/10.1093/rfs/hhw101>
- Barillas, F., & Shanken, J. (2018). Comparing asset pricing models. *The Journal of Finance*, 73(2), 715–754. <https://doi.org/10.1111/jofi.12607>
- Kozak, S., Nagel, S., & Santosh, S. (2018). Interpreting factor models. *The Journal of Finance*, 73(3), 1183–1223. <https://doi.org/10.1111/jofi.12612>
- Cattaneo, M. D., Crump, R. K., Farrell, M. H., & Schaumburg, E. (2020). Characteristic-sorted portfolios: Estimation and inference. *The Review of Economics and Statistics*, 102(3), 531–551. https://doi.org/10.1162/rest_a_00883
- Jensen, T. I., Kelly, B., & Pedersen, L. H. (2023). Is there a replication crisis in finance? *The Journal of Finance*, 78(5), 2465–2518. <https://doi.org/10.1111/jofi.13249>
- Giglio, S., Xiu, D., & Zhang, D. (2025). Test assets and weak factors. *The Journal of Finance*, 80(1), 259–319. <https://doi.org/10.1111/jofi.13415>
- Shin, U. (2026a). Which portfolios? The construction dependence of factor model performance. *arXiv preprint arXiv:2606.19550*. <https://doi.org/10.48550/arXiv.2606.19550>

- Shin, U. (2026b). Anatomy of the Market: A Body-Tail Test of Factor Models. *arXiv preprint arXiv:2606.23596*. <https://doi.org/10.48550/arXiv.2606.23596>
- Jegadeesh, N., & Titman, S. (1993). Returns to buying winners and selling losers: Implications for stock market efficiency. *The Journal of Finance*, 48(1), 65–91. <https://doi.org/10.1111/j.1540-6261.1993.tb04702.x>
- Carhart, M. M. (1997). On persistence in mutual fund performance. *The Journal of Finance*, 52(1), 57–82. <https://doi.org/10.1111/j.1540-6261.1997.tb03808.x>
- Fama, E. F., & French, K. R. (1992). The cross-section of expected stock returns. *The Journal of Finance*, 47(2), 427–465. <https://doi.org/10.1111/j.1540-6261.1992.tb04398.x>
- Fama, E. F., & French, K. R. (1993). Common risk factors in the returns on stocks and bonds. *Journal of Financial Economics*, 33(1), 3–56. [https://doi.org/10.1016/0304-405X\(93\)90023-5](https://doi.org/10.1016/0304-405X(93)90023-5)
- Fama, E. F., & French, K. R. (2015). A five-factor asset pricing model. *Journal of Financial Economics*, 116(1), 1–22. <https://doi.org/10.1016/j.jfineco.2014.10.010>
- Fama, E. F., & French, K. R. (2018). Choosing factors. *Journal of Financial Economics*, 128(2), 234–252. <https://doi.org/10.1016/j.jfineco.2018.02.012>
- Hou, K., Xue, C., & Zhang, L. (2015). Digesting anomalies: An investment approach. *The Review of Financial Studies*, 28(3), 650–705. <https://doi.org/10.1093/rfs/hhu068>
- Hou, K., Mo, H., Xue, C., & Zhang, L. (2019). Which factors? *Review of Finance*, 23(1), 1–35. <https://doi.org/10.1093/rof/rfy032>
- Hou, K., Xue, C., & Zhang, L. (2020). Replicating anomalies. *The Review of Financial Studies*, 33(5), 2019–2133. <https://doi.org/10.1093/rfs/hhy131>
- Hou, K., Mo, H., Xue, C., & Zhang, L. (2021). An augmented q-factor model with expected growth. *Review of Finance*, 25(1), 1–41. <https://doi.org/10.1093/rof/rfaa004>
- Hou, K., Mo, H., Xue, C., & Zhang, L. (2024). The economics of security analysis. *Management Science*, 70(1), 164–186. <https://doi.org/10.1287/mnsc.2022.4640>
- Center for Research in Security Prices, LLC. (2026). *CRSP US Stock Databases* [Data set]. Accessed via Wharton Research Data Services, June 5, 2026. <https://www.crsp.org/research/>
- French, K. R. (2026). *Kenneth R. French Data Library* [Data set]. Accessed May 5, 2026. https://mba.tuck.dartmouth.edu/pages/faculty/ken.french/data_library.html
- Global-q.org. (2026). *Factors and testing portfolios* [Data set]. Accessed May 5, 2026. <https://global-q.org/factors.html>
- Global Factor Data. (2026). *Global Factor Data* [Data set]. Accessed June 28, 2026. <https://jpkpfactors.com>